DYNAMIC MODES IN TURBULENT CAVITY FLOWS CAUSING SELF-SUSTAINED OSCILLATIONS

Abu Seena and Hyung Jin Sung
Department of Mechanical Engineering, KAIST
291 Daehak-ro, Yuseong-gu, Daejeon, 305-701, South Korea
abuseena@kaist.ac.kr, hjsung@kaist.ac.kr

ABSTRACT

Large eddy and direct numerical simulations of incompressible turbulent flows were performed over an open cavity with or without self-sustained oscillations possessing thin or thick incoming boundary layers ($Re_D = 12000$ and 3000). The influence of the incoming turbulent boundary layer on the cavity was investigated using dynamic mode decomposition (DMD). The cavity length to depth ratio of 2 was selected for both cases. In the case of thick boundary layer, the dynamic modes extracted using the DMD algorithm shows that the upcoming boundary layer structures and the structures generated due to the shear layer oscillations differs in wavelength space. The upcoming BL structures larger than the cavity dimensions convect over the cavity. On the other hand, in the case of thin boundary layer both of the upcoming and the shear layer structures possess comparable dimensions. This may lead to the condition of resonance causing self-sustained oscillations. This result suggests that the hydrodynamic resonance causing self-sustained oscillations occur when the upcoming boundary layer structures and shear layer structures coincide both in the frequency and wavenumber space. The structures of the cavity perturbations change with the cavity size and upcoming momentum thickness.

INTRODUCTION

In turbulent cavity flows, the coherent features are observed along the shear layer possessing wide range of wavenumbers. However, in many situations, the flow complexity actually reduces to very coherent features together with few characteristic structures possessing self-excited global modes in space and time. The dynamic information becomes quite significant in the cases where the local absolute instability prevails in the finite region. In such situations, the systems may exhibit self-sustained resonant modes at specific complex frequencies. The global stability analysis results in large stability matrix size and implying the Arnoldi method it may be computationally expensive due to iterative schemes adopted. Schmid (2010) introduced a method known as dynamic mode decomposition (DMD) to extract dynamic mode information from the flow fields. The extracted dynamic modes, which may be interpreted as a generalization of global stability modes, can be used to describe the underlying physical mechanism captured in the data sequence. The mathematics underlying this decomposition is related to the Koopman operator which provides a linear representation of a nonlinear dynamical system (Rowley *et al.* 2010).

Flows over an open cavity occur in many engineering applications, for example landing gear wells and bomb bays in aircraft and sunroofs in automobiles. The presence of the open cavity generates strong self-sustained oscillations of velocity, pressure and, occasionally, density. To understand the mechanism underlying such oscillations and prevent undesirable effects, numerous experimental and numerical studies have been carried. Pereira & Sousa (1995) observed periodically oscillating shear layers in the flow of a turbulent incoming boundary layer over an open cavity. Lin & Rockwell (2001) also observed self-sustained oscillations in water-tunnel experiments, and suggested that the oscillations are related to large-scale vortical structures. Chatellier, Laumonier & Gervais (2004) observed self-sustained oscillations of the mixing layer in their experiments, and suggested that the oscillating process is not governed by periodic shedding of coherent structures but by convective waves of naturally unstable mixing layer. However, Ashcroft & Zhang (2005) observed the shedding of large-scale vortical structures by Galilean decomposition of the instantaneous and fluctuating velocity fields. The coherent vortical structures were present in the majority of PIV images, although well-defined structures were not always observed. The authors pointed out small peaks in the pressure spectra as evidence of weak tonal components; however strong self-sustained oscillations were not observed. The work of Lee *et al.* (2008) was the large eddy simulation (LES) of high-Reynolds number incompressible turbulent flows over an open cavity. An analysis of raw data, including instantaneous velocity or vorticity distributions, usually requires that structural analysis of separated shear layers is instantaneous and qualitative. Therefore, application of an analysis approach such as DMD is required for a quantitative and dynamic characterization of large-scale vortical structures. The objectives of the present study are to identify large-scale vortical structures responsible for hydrodynamic oscillations by employing the DMD to the pressure fluctuations of incompressible turbulent flows over an open cavity; and obtain the dynamic information of the extracted structures. To elucidate the quantitative characteristics of large-scale vortical structures, the oscillating behaviours of a separated shear layer are compared with those of a non-oscillating system. The two different data of cavity flows ($Re_D = 12000$ and 3000) with and without self-sustained

oscillations have been analyzed under the influence of upstream thin and thick boundary layers (Re_θ = 300 and 670), respectively.

DYNAMIC MODE DECOMPOSITION

Dynamic mode decomposition is a recent extension of the classical Arnoldi technique. A temporal sequence of N data fields, consisting of column vectors, $\mathbf{v}_j$, that are equispaced in time, can be written as

$$\mathbf{V}_1^N = \{\mathbf{v}_1, \ \mathbf{v}_2, \ \mathbf{v}_3, \ldots\ldots, \ \mathbf{v}_N\}. \tag{1}$$

The basic premise of the method is that each snapshot in time is assumed to be generated by a linear dynamical system, $\mathbf{v}_{j+1} = \mathbf{A}\mathbf{v}_j$. The eigenvalues and eigenvectors of the matrix A completely characterize the behaviour of the dynamical system. DMD is a method for computing the approximate eigenvectors or Ritz vectors of a system matrix. A high-degree polynomial is fit to a Krylov sequence of flow fields. As the number of snapshots increases, the flow is assumed to approach a linear dependency after a sufficient number of snapshots such that the last image is the linear combination of the previous images. It represents an over-determined system of equations. The coefficients may be obtained using the least squares method. The number of required snapshots, N, may increase until the residual converges. Following Ruhe (1984), the least squares description of the full system matrix A may be written as

$$\mathbf{A}\mathbf{V}_1^{N-1} = \mathbf{V}_2^N = \mathbf{V}_1^{N-1}\mathbf{C} + \mathbf{r}\mathbf{e}_{N-1}^T. \tag{2}$$

The matrix C is of the companion type which simply shifts the snapshot index from 1 through N–1. This matrix, extracted from the data sequence, represents a low-dimensional system matrix representation of the full system matrix. The characteristic solution to the matrix C approximates some of the eigenvalues (λ_j) of the full system matrix A. These eigenvalues provide the growth and frequency information. The empirical Ritz values lying on the unit circle represent the modes with zero growth rate, whereas the eigenvalues lying inside and outside the unit circle represent the damped and undamped modes respectively. The eigenvectors provide a linear combination of basis coefficients that may be used to extract the corresponding dynamic modes as,

$$\boldsymbol{\Phi}_j = \mathbf{V}_1^{N-1}\mathbf{T}_j. \tag{3}$$

To attain the time behaviour of each dynamic mode, the coefficients may be shifted along the data sequence.

The companion matrix may be a highly non-normal matrix, which yields an ill-conditioned eigenvalue decomposition problem. To improve the accuracy of the DMD method, Bagheri (2010) suggested that the matrix should first be balanced by a similarity transformation, followed by reducing to an upper Hessenberg form via a second similarity transformation, and finally, the eigenvalues should be computed using the QR algorithm. In the present work, the modifications proposed by Bagheri (2010) were included. The modes ($\boldsymbol{\Phi}_j$) of the companion matrix were constructed from the data sequence $\mathbf{V}_1^{N-1}$, and its L2-norm yielded the energy of the respective modes, which were found to be representative of the scales of the turbulence in the cavity flows.
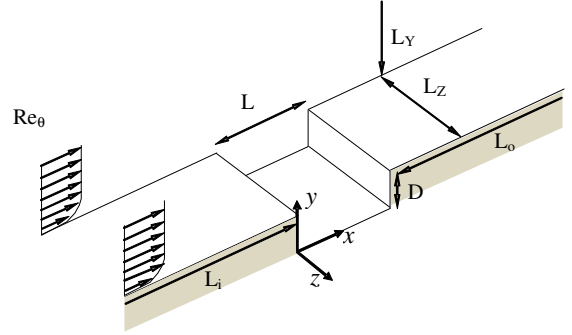
Figure 1. Schematic diagram of the computational domain.

NUMERICAL SIMULATION

For an incompressible flow, the non-dimensional governing equations are

$$\frac{\partial u_i}{\partial t} + \frac{\partial u_i u_j}{\partial x_j} = -\frac{\partial p_i}{\partial x_i} + \frac{1}{Re_D}\frac{\partial^2 u_i}{\partial x_j^{\,2}}, \quad i = 1,2,3 \tag{4}$$

$$\frac{\partial u_i}{\partial x_i} = 0, \tag{5}$$

where x_i are the Cartesian coordinates and u_i are the corresponding velocity components. The free-stream velocity U_∞ and the cavity depth D were used to non-dimensionalize the equations. The Reynolds number was defined as $Re_D = U_\infty D/v$, where v is the kinematic viscosity. The governing equations (4) and (5) were integrated in time using the fully implicit decoupling method proposed by Kim et al. (2002). A schematic diagram of the computational domain is shown in Figure 1. In the present simulations, a turbulent boundary layer with realistic velocity fluctuations, which were generated using the method of Lund et al. (1998), was provided at the inlet. Two cavity flow data sets, with or without self-sustained oscillations and possessing thin or thick incoming boundary layers (Re_D = 12000 and 3000), were simulated. The ratios between the cavity depth and the momentum thickness (D/θ) were 40 and 4.5, respectively, and the cavity aspect ratio was L/D = 2. A direct numerical simulation (DNS) of incompressible flows over an open cavity was performed at Re_D = 3000, where the DNS data were provided at the inlet with Re_θ = 670. The cavity flows at high Reynolds number (Re_D =12000) were simulated using a large eddy simulation (LES) with a dynamic subgrid-scale model. The simulation conditions used in the present study are summarized in Table 1. The computational details are given in Lee et al. (2010).

Table 1 Simulation conditions.

Re_D	Re_θ	$N_x \times N_y \times N_z$	Δx_{min}^+, Δx_{max}^+	Δy_{min}^+
3000	670	513×213×257	1.09, 17.7	0.18
12000	300	897×169×257	1.4, 40	0.56
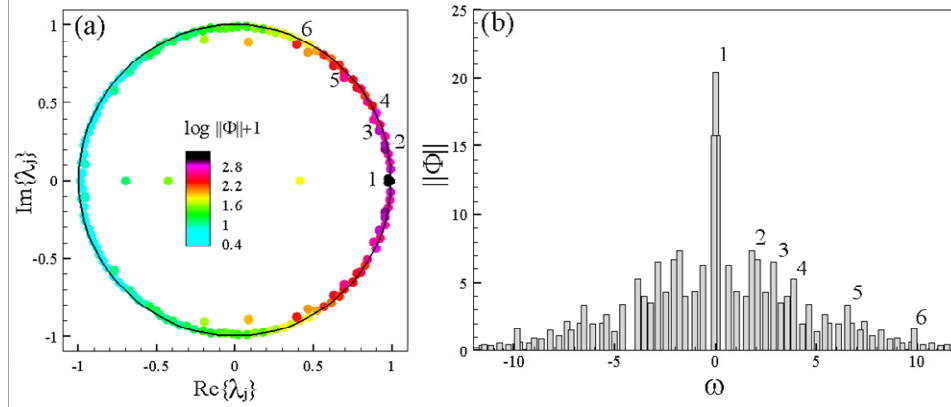
Figure 2. Ritz values λ_j and their magnitudes at $Re_D = 3000$.
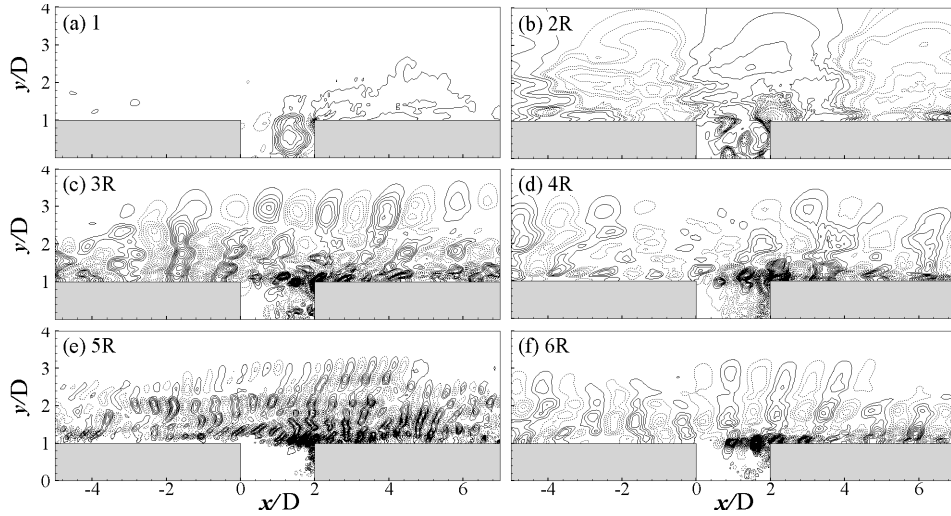
Figure 3. DMD modes inside the cavity full domain at $Re_D = 3000$.

RESULTS AND DISCUSSION

The flows corresponding to each of the two cases considered in the present study, $Re_D = 3000$ and 12000, were simulated. After a long initial transient period, a sequence of images was saved. An initial transient time of more than 10 "flow-through" cycles was discarded to allow the passage of unphysical fluctuations. Nevertheless, the snapshots by themselves do not represent an objective and quantitative means to gain insight into the prevalent perturbation dynamics. Moreover, only the most dominant features can be observed, whereas more subtle and smaller-scale instabilities may be missed. For this reason, the temporal sequences of the system snapshots were processed using the DMD algorithm to extract pertinent dynamic characteristics of the flow. The algorithm is applied over the entire physical domain, including both the upstream region of the leading edge and the downstream region of the trailing edge. The sequences of

pressure snapshots equi-spaced in time are processed. One hundred fifty instantaneous snapshots of the pressure fluctuations were used for the $Re_D = 3000$ condition, and 124 snapshots were used for the $Re_D = 12000$ condition. The residuals rapidly converged over these images, and the eigenvalues of the subspace C were expected to converge toward some of the eigenvalues of the full system matrix A.

A. $Re_D = 3000$ and $D/\theta = 4.5$

The flow fields for cavity with thick incoming boundary layer at each of the 150 time-step will be reshaped into the columns of a data matrix V_1^{150}. The empirical Ritz values $\boldsymbol{\lambda}_j$ and the empirical Ritz vectors $\mathbf{T}_j$ of a sequence of flow fields V_1^{150} are computed using the algorithm described earlier. The eigenvalues extracted from the low-dimensional matrix $\mathbf{C}$ is shown in Fig. 2(a), where the symbol color indicates norm of mode. Nearly all the Ritz values are on the unit circle $\|\lambda_j\| = 1$,

indicating that the sample points vi lie on or near an attracting set. The norm of each mode indicates the energy in the corresponding mode. The energies of the extracted modes are shown as a function of frequency in Fig. 2(b), where each mode is displayed with the vertical line scaled with its magnitude at its corresponding frequency. The eigenvalues obtained over a low-dimensional subspace were found to be in complex conjugate pairs. As a result, the DMD spectrum was symmetric about the frequency $\omega = 0$, as shown in Fig. 2(b). The eigenvalue marked 1 that typically appears at the origin ($\omega = 0$) with the maximum energy accounts for the steady state and represents the mean flow as such depicted by a black symbol in Fig. 2(a). The corresponding dynamic mode is shown in Fig. 3(a), where the low-pressure region observed in the cavity indicates the primary vortex. A high-pressure region is also observed at the trailing edge, possibly due to the impingement of shear layer vortical structures. Five distinct frequency peaks are marked 2–6, and their corresponding modes are shown in Figs. 3(b)–(f). The eigenvalue marked 2 in the spectrum indicates a very low frequency mode. The pressure fluctuations of the corresponding mode, shown in Fig. 3(b), indicate the presence of a very large-scale structure relative to the size of the cavity which convects over the cavity. The mode marked 3 is shown in Fig. 3(c). In addition to the upcoming boundary layer structures, the structures generated due to shear layer oscillations could be observed along the cavity lip line, which further impinged on the trailing edge. The eigenvalue marked 4 is shown in Fig. 3(d). The structures that appear in this particular mode suggest that at this frequency, the wavenumber corresponding to the upcoming boundary layer structure and the perturbation generated by shear layer oscillations are equal. The modes of two other eigenvalues marked 5 and 6 are displayed in Figs. 3(e) and 3(f). The modes observed in all Figs. 3(b)–(f) correspond to the structures of the upcoming boundary layer. Note that all the modes in Fig. 10 represent the incoming viscous boundary layer structures.

B. $Re_D = 12000$ and $D/\theta = 40$

LES of incompressible cavity flow over an open cavity were performed at $Re_D = 12000$. Realistic velocity fluctuations of $Re_\theta = 300$ were provided at the inlet. One hundred twenty-four

images of the instantaneous pressures were processed using the DMD algorithm, and a low-dimensional subspace was extracted. The extracted spectrum, i.e., the spectrum of C, is displayed in Fig. 4(a), where all the Ritz values are on the unit circle. The symbol color indicate the global energy norms of the modes. The spectra displayed a dominant peaks, marked 2 and 4 with two leading modes at ω= 3.5 Hz and 4.6 Hz respectively.   Some of the selected modes from the spectrum in Fig. 4(b), marked 1–4, are shown in Fig. 5(a)-(d). The eigenvalue at the origin, marked 1 in the spectrum, represents the steady state component of the pressure, and its respective mode is shown in Fig. 5(a). The modes marked 2 and 3 with dominant peak are shown in Figs. 5(b) and 5(c) respectively. One pair of negative and positive distributions represents the low-pressure fluctuations of a large-scale vortical structure and the high-pressure fluctuations of induced rotational motions. Three pairs are clearly observed between the leading and trailing edges. This was consistent with the spectral characteristics of self-sustained oscillations corresponding to N_R=3, reported by Lee *et al.* (2008). The streamwise length scale of the coherent structures gradually increases from 0.3D in the region immediately downstream of the leading edge to 0.8D in the region that impinges on the trailing edge. To avoid ambiguity, the length scale of the coherent structure was determined to be twice as long as the streamwise distance between the central locations of the positive and negative distributions. The transverse length scale was not sufficiently large to affect the pressure fluctuations on the bottom wall inside the cavity. These modes suggest the presence of self-sustained oscillations in the cavity. The symbol marked 4, and its respective mode is shown in Fig. 5(d).

The size of structures along the shear layer is comparable to that of the upstream boundary layer structures. The modes in Figs. 5(b)–(d) indicate that the structures along the shear layer coincide with the wavenumber spectra of the upstream boundary layer structures. This coincidence may have produced self-resonant modes. Although alternating pressure fluctuation patterns were regularly observed in the first and second modes, the distributions in the other modes were irregular. The other modes most likely describe the fluctuating behaviour of a separated shear layer with a high wavenumber, albeit with slight variations. In previous studies of laminar cavity flows, the oscillating behaviour of a separated shear
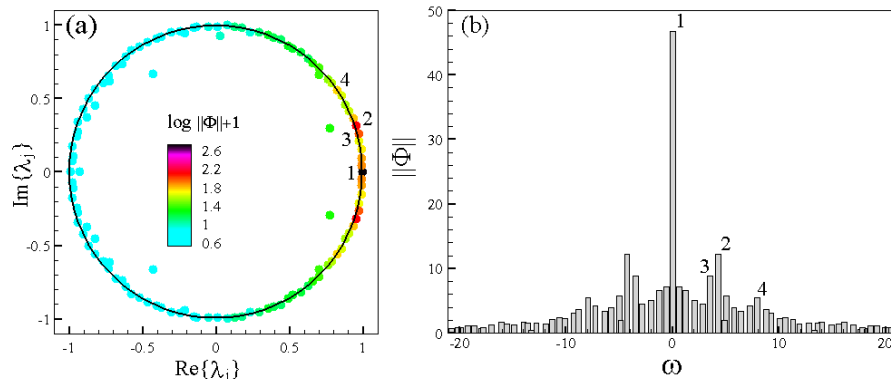
Figure 4. Ritz values λ_j and their magnitudes at $Re_D = 12000$

4
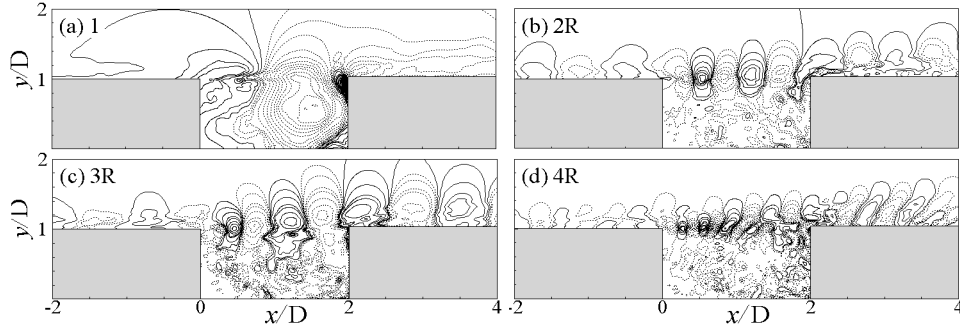
Figure 5. DMD modes inside the cavity full domain at $Re_D = 12000$.

layer was represented only by the first two modes, whereas the next higher modes were associated with recirculation of the primary vortex inside the cavity. The simple modes of a separated shear layer produce a single peak frequency in the power spectra of laminar cavity flows. In the present study of turbulent cavity flows, however, the fluctuating behaviour of the separated shear layer was represented in the higher modes as well as in the first two modes. The complex mixture of several modes produces a broad spectrum, corresponding to the pressure fluctuations in the fluctuating behaviour of the separated shear layer, although the first two modes are responsible for the peak frequency corresponding to $N_R = 3$.

For each mode, the average wavelength of the structures was measured along the shear layer. To avoid ambiguity, the wavelength (λ_x) of the coherent structure was determined to be twice as long as the streamwise distance between the central locations of the positive and negative distributions. Figure 6 plot the wavelength as a function of the frequency for both cases. The DMD algorithm extracted a wide range of structures. We found that the large structures were associated with lower frequencies, and the frequency increased as the wavelength of the structures decreased. This result agrees well with equation Rossiter's equation, which describes the wavelength as the reciprocal of the frequency of structures with the same convection velocity. Figure 6 show the frequency on a log–log scale. The slope –1 indicates that the wavelength and frequency follow a reciprocal relationship. A drop in the frequency was observed for those structures with a

smaller scale. This drop in frequency may have been due to the presence of small-scale structures along the shear layer in the high velocity gradient region and, hence, the shear layer may be characterized by a lower convection velocity. In both cases, $Re_D = 3000$ and 12000, the reciprocal law holds well for structures larger than the wavelength $\lambda_x /D= 0.2$. This suggests that structures larger than $\lambda_x /D= 0.2$ convect downstream with the same velocity.

All modes extracted using the DMD algorithm indicated that the flow was characterized by turbulent structures. The L2-norm of the modes yielded the energies in the associated modes. The energy ($\|\Phi\|$) is plotted against wavenumber on a log–log scale in Fig. 7 for both cases analyzed in the present work. The Kolmogorov power law (–5/3) is also plotted (solid line) in the same figure. The high value of the power law prefactor at $Re_D = 12000$ shows that it contains higher energy modes than the cavity flow at $Re_D = 3000$. The region in which the data agree well with the Kolmogorov power law corresponds to the turbulence cascade region called the inertial range. The inertial range was broader for the higher Reynolds number flows, $Re_D = 12000$, than for the thick boundary layer flow ($Re_D = 3000$). The modes extracted using the DMD algorithm showed a turbulent energy cascade, thus supporting the turbulent nature of the flow.

CONCLUSIONS

In the present study, we identified large-scale vortical

Figure 6. Wavelength of structure against frequency.
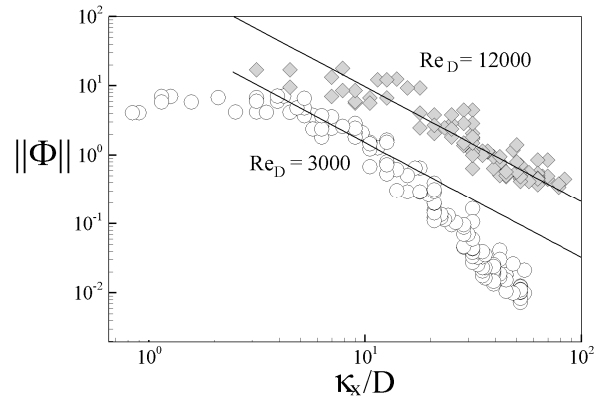
Figure 7. Wavenumber spectrum.

structures responsible for self-sustained oscillations by employing a dynamic mode decomposition of the pressure fluctuations of turbulent flows over an open cavity. DMD was applied to incompressible turbulent flows over an open cavity at Re_D = 3000 and 12000, with upstream turbulence of Re_θ = 670 and 300, respectively, provided at the inlet. The influence of the incoming turbulent boundary layer on the self-sustained oscillations was investigated. A wide range of structures was extracted using the DMD algorithm. The dynamic information obtained from DMD algorithm identified the dynamic mode and its behaviour in time. The cavity with thick incoming boundary layer represented the viscous boundary layer structures, whereas the thin incoming boundary layer showed a dominant peak in the spectrum which represented the cavity dynamics. A mode with the dominant peak in DMD spectrum at Re_D = 12000 represents the structure responsible for self-sustained oscillations. This mode shows three pairs of alternating patterns of pressure fluctuations. These structures were consistent with the spectral characteristics of self-sustained oscillations corresponding to N_R = 3. The dynamic modes extracted from the thick boundary layer (Re_D = 3000) showed that both the boundary layer structures and the shear layer structures coexist in similar frequency space but with different wavenumber space. These results suggest that the hydrodynamic resonance that produces self-sustained oscillations occurs when the upcoming boundary layer structures and the cavity shear layer structures coincide not only in frequency space, but also in wavenumber space. Hence, the upcoming boundary layer thickness was found to be a significant parameter for describing self-sustained oscillations. The parameter D/θ for flows over an open cavity, was, therefore, found to be important. The DMD energy spectra agreed well with the Kolmogorov power law, supporting the conclusion that the extracted modes represent the turbulence scales.

REFERENCES

Akervik, E., Hoepffner, J., Ehrenstein, U., and Henningson, D. S. , 2007, "Optimal growth, model reduction and control in a separated boundary-layer flow using global modes", *J. Fluid Mech*. Vol. 579, pp. 305–314.

Ashcroft, C., and Zhang, X., 2005, "Vortical structures over rectangular cavities at low speed", *Phys. Fluids*, Vol. 17, 015104 .

Bagheri, S., 2010, "Analysis and control of transitional shear flows using global modes" *PhD Thesis*, February, Dept. of Mechanics, Royal Institute of Technology, Sweden.

Chatellier, L., Laumonier, Y. and Gervais, Y., 2004, "Theoretical and experimental investigations of low Mach number turbulent cavity flows", *Experiments of Fluids*, Vol. 36, pp. 728-740.

Kim, K., Baek, S.-J., and Sung, H.J., 2002, "An implicit velocity decoupling procedure for the incompressible Navier-Stokes equations", *Intl. J. Numer. Meth. Fluids*. Vol. 38 (2), pp 125-.

Lee, S.B., Kang, W., and Sung, H.J., 2008, "Organized self-sustained oscillations of turbulent flows over an open cavity", *AIAA J.,* Vol. 46(11), pp. 2848-2856.

Lee, S.B., Seena, A., and Sung, H.J., 2010, "Self-sustained oscillations of turbulent flow in an open cavity", *J. Aircraft* Vol. 47(3), pp. 820-834.

Lin, J.-C., and Rockwell, D. 2001, "Organized oscillations of initially turbulent flow past a cavity", *AIAA J.* , Vol. 39 (6), pp. 1139-1151.

Lund, T.S., Wu, X., and Squires, K.D., 1998, "Generation of turbulent inflow data for spatially-developing boundary layer simulation", *J. Comp. Phy.,* Vol. 140, pp. 233-258.

Pereira, J.C.F., and Sousa, J.M.M., 1995, "Experimental and numerical investigation of flow oscillations in a rectangular cavity", *J. Fluids Engng.,* Vol. 117, pp. 68-74.

Rowley, C.W., I. Mezic, I., Bagheri, S., Schlatter, P., and Henningson, D.S., 2009, "Spectral analysis of nonlinear flows", *J. Fluid Mech.,* Vol. 641, pp. 115-127.

Ruhe, A., 1984, "Rational Krylov sequence methods for eigenvalue computation", *Lin. Alg. App.* Vol. 58, pp. 279-316.

Schmid, P.J., 2010, "Dynamic mode decomposition of numerical and experimental data", *J. Fluid Mech*. Vol. 656, pp. 5-28.

Sipp, D. and Lebedev, A. 2007 "Global stability of base and mean flows: a general approach and its applications to cylinder and open cavity flows", *J. Fluid Mech.,* Vol. 593, pp. 333–358.